A 4,096-Channel Current-Clamp CMOS Neural Interface with Overlay and Shank Electrodes

Yuchang Zhang[1,*], Jun Wang[1,*], Hefei Liu[1,*], Nadir Talha[1], Luis E. Boero[2], Venkatesh N. Murthy[2], Donhee Ham[1]

[1]Harvard John A. Paulson School of Engineering and Applied Sciences, Harvard University, Cambridge, MA, USA

[2]Department of Molecular and Cellular Biology, Harvard University, Cambridge, MA, USA

*Equal contribution. Email: Donhee@seas.harvard.edu

Surface-overlay microelectrode arrays (MEAs) on CMOS chips are a central platform for population-scale extracellular recording from *in vitro* neuronal networks [1,2]. Recently, the platform saw two major extensions. First, current-clamp operation at each electrode—simultaneous current injection to permeabilize the membrane for intracellular access and voltage recording—enabled population-scale intracellular recording *in vitro* [3–5]. It supports intracellular recording with current injection on while retaining conventional extracellular recording with current injection off, collectively forming an intracellular MEA (iMEA) class of architectures [5]. Second, electrodes were monolithically routed away from the active circuitry, and the remote electrode array region was etched into brain-insertable shanks, enabling high-density population-scale extracellular recording *in vivo* [6,7].

We present a CMOS neural interface chip that combines these two extensions—the iMEA and shank technologies (Fig. 1). On the one hand, it integrates 4,096 current-clamp analog front-end (AFE) channels, enabling iMEA-class operation that supports both intracellular and extracellular recording modalities. On the other hand, it integrates shank-embedded *in vivo* electrodes in addition to surface-overlay *in vitro* electrodes. An integrated switching network steers the AFE channels to either electrode type. This chip thus provides, for the first time, a hardware platform for the four combinations of recording modality and environment at population scale: extracellular/intracellular *in vitro* and extracellular/intracellular *in vivo*.

We use the chip to record, also for the first time, in three of these combinations: extracellular and intracellular recordings from rat cortical neurons *in vitro*, and extracellular recordings from the mouse olfactory bulb *in vivo*. The fourth combination—population-scale intracellular recording *in vivo*—remains an open challenge in the field, due so far to both the lack of a hardware platform and biological barriers such as immune response. This work provides that missing hardware platform, narrowing the challenge to the biological interface.

The chip is realized in a 180-nm CMOS process. The two types of electrode arrays—a 4,096 surface-overlay electrode array for *in vitro* work and a 2,048 remotely-routed electrode array for *in vivo* work—are built on foundry-fabricated metal pads via post-fabrication processing (Fig. 1). The remotely-routed electrode array region is etched into brain-insertable shanks, also during post-fabrication.

The 4,096 current-clamp AFE channels are integrated with 64 12-bit SAR ADCs. The AFE channels are organized into 64 groups, each with 64 channels time-multiplexed to one ADC (Fig. 1).

Each current-clamp AFE channel comprises a current injector for intracellular access and a configurable amplifier for voltage recording, enabling iMEA-class operation (Fig. 2a). The amplifier is based on a folded-cascode operational transconductance amplifier (OTA) (Fig. 2b) with switches in the input and feedback paths for various amplification modes (Fig. 2a). For example, the amplifier can be configured in a high-gain mode (~400 V/V) for low-amplitude extracellular signals with current injection off, or in a low-gain mode (~30 V/V) for high-amplitude intracellular signals with current injection on (Fig. 2c). Fig. 2d shows the measured gain-versus-frequency responses for these two configurations.

The current injector in each AFE channel has two selectable schemes (Fig. 2a). The first is a switched-capacitor current injector, where a limited number of array-shared current levels—each finely tunable over a wide range—are available at a given time [3]. The second is a DRAM-style current injector (DCI), which enables independent per-channel current programming. The DCI generates per-channel current by storing an analog voltage on a local capacitor that biases a PMOS transistor (Fig. 3a). By tuning this capacitor voltage, the PMOS transistor is biased across the subthreshold and saturation regimes, allowing the DCI output current to span from pA to μA range (Fig. 3b). One external DAC sequentially programs the DCI capacitor voltages across all 4,096 channels, each of which is refreshed every ~20 ms to compensate for charge leakage. Fig. 3c shows independent current programmability across channels. Fig. 3d shows a spatially programmed current pattern across the array.

The switching network comprises input selection switches and inter-channel connection switches (Fig. 4a). The input-selection switches are used to connect the same current-clamp AFE channels to either the 4,096 surface-overlay *in vitro* electrodes or the 2,048 shank-embedded *in vivo* electrodes. This allows the same iMEA-class front-end to operate across both *in vitro* and *in vivo* environments.

The inter-channel switches provide a second function. While AFE channels can operate independently, each reading from its individually assigned electrode, the inter-channel switches can join multiple adjacent AFE channels by shunting their amplifier inputs, enabling the formation of local AFE clusters that collectively record from a common electrode (Fig. 4b). In this local clustering scheme, the outputs of the clustered AFE channels receiving the same input are averaged to reduce uncorrelated amplifier and digitization noise, resulting in improved SNR, at the expense of spatial resolution (i.e., some electrodes are not assigned to AFEs for recording) (Fig. 4c). The AFE clusters can remain assigned to selected electrodes to improve their SNR, or be reassigned over time to scan across the array to improve SNR across the electrode set.

For *in vitro* experiments, rat cortical neurons were cultured on the surface-overlay electrode array of the open-packaged CMOS chip. In extracellular recording mode, AFEs operate at high gain with current injection off. Over 800 of 4,096 channels detected >100 spikes over 5 min of recording, with spike amplitudes of 200–300 μV at electrodes (Fig. 5a, top). Clustering 9 AFEs yielded a ~6 dB SNR improvement in extracellular recording, indicating that ~80% of the noise is uncorrelated (Figs. 5c and 5d). Separately, in intracellular recording mode, AFEs operate at low gain with current injection for membrane permeabilization. Spike amplitudes increased to the mV range with polarity inversion (e.g., ~9 mV, Fig. 5a, bottom).

For *in vivo* experiments (Fig. 5b), of four shanks with 512 electrodes each, three were inserted into the olfactory bulb of a mouse (one was broken). Of these, ~768 electrodes were positioned within tissue due to partial insertion depth. Across extracellular recording sessions, 72–126 electrodes registered spikes, yielding 51–88 sorted units.

Fig. 6 shows performance comparison. Fig. 7 shows the chip micrograph and power consumption breakdown.

Acknowledgements:

We acknowledge support from the Gates Foundation (INV-089977) and Samsung Electronics SAIT (A59707, A37734).

References:

[1] U. Frey et al., “Switch-Matrix-Based High-Density Microelectrode Array in CMOS Technology,” IEEE J. Solid-State Circuits, vol. 45, no. 2, pp. 467–482, Feb. 2010.

[2] J. Dragas et al., “In Vitro Multi-Functional Microelectrode Array Featuring 59 760 Electrodes, 2048 Electrophysiology Channels, Stimulation, Impedance Measurement, and Neurotransmitter Detection Channels,” IEEE J. Solid-State Circuits, vol. 52, no. 6, pp. 1576–1590, Jun. 2017.

[3] J. Abbott et al., “The Design of a CMOS Nanoelectrode Array With 4096 Current-Clamp/Voltage-Clamp Amplifiers for Intracellular Recording/Stimulation of Mammalian Neurons,” IEEE J. Solid-State Circuits, vol. 55, no. 9, pp. 2567–2582, Sep. 2020.

[4] J. Abbott et al., “A nanoelectrode array for obtaining intracellular recordings from thousands of connected neurons,” Nat Biomed Eng, vol. 4, no. 2, pp. 232–241, Sep. 2019.

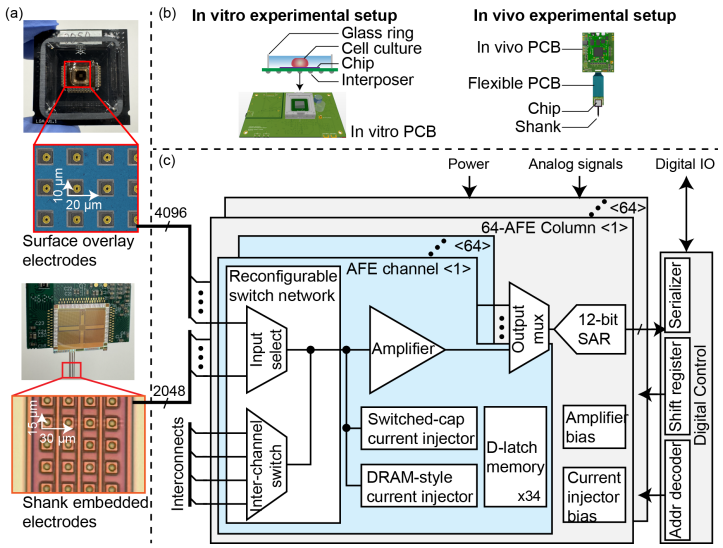


Fig. 1. (a) Same chip differently packaged for *in vitro* and *in vivo* use. (b) *In vitro* and *in vivo* experimental setups. (c) Chip block diagram.

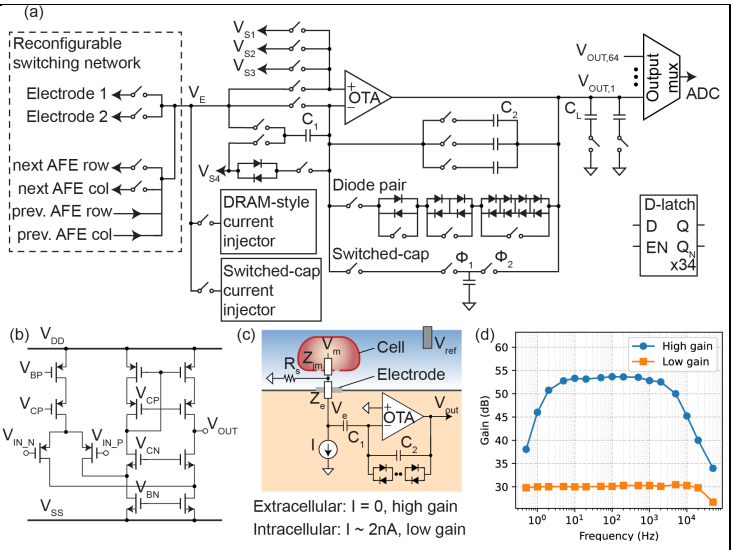


Fig. 2. (a) Current-clamp AFE channel. (b) OTA. (c) AFE channel configurations for extracellular & intracellular (high- & low-gain) modes. (d) Measured AFE amplifier gain vs. freq. for the two modes.

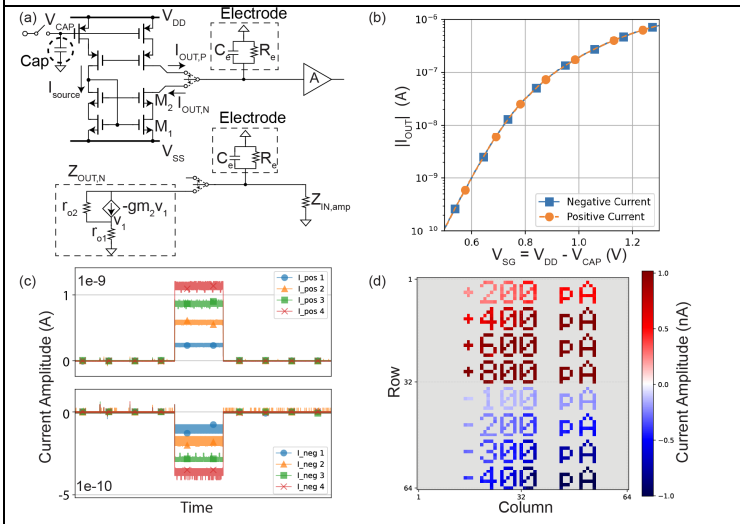


Fig. 3. (a) DCI circuit schematic. (b) Measured DCI output current vs. capacitor voltage. (c) Measured DCI current pulses from multiple channels. (d) Heatmap of a programmed DCI current pattern across the surface-overlay electrode array.

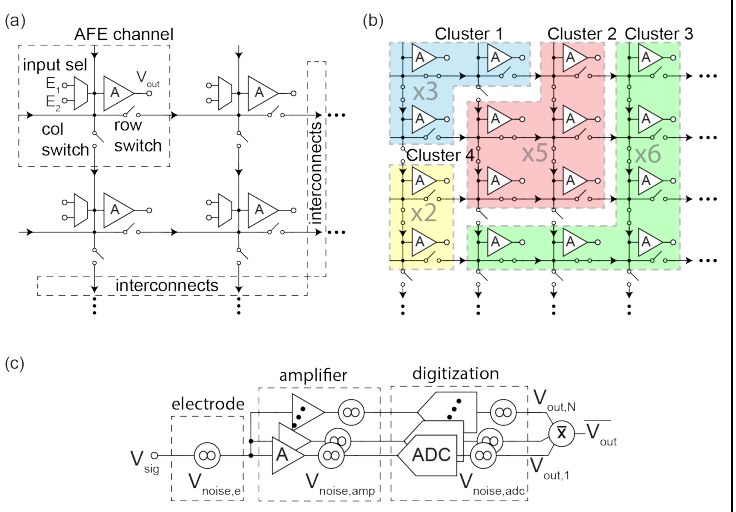


Fig. 4. (a) Switching network architecture. (b) Formation of local AFE clusters. (c) Signal averaging of locally clustered AFE outputs.

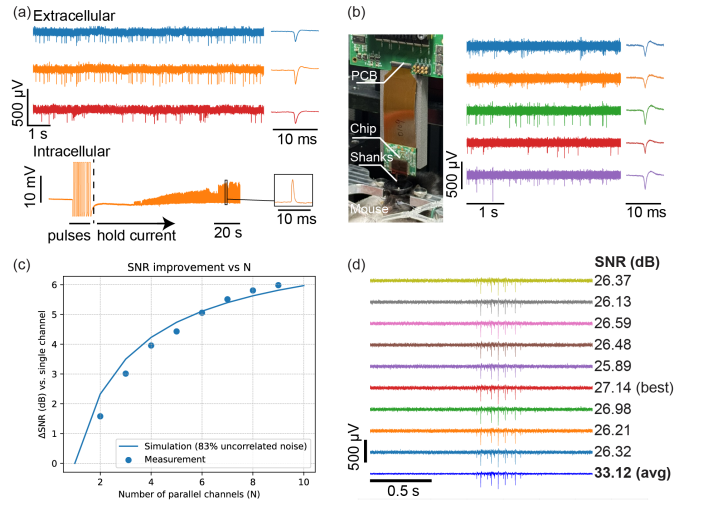


Fig. 5. (a) Extracellular/intracellular recording traces; rat neurons *in vitro*. (b) Extracellular traces; mouse olfactory bulb *in vivo*. (c) Simulated/measured SNR increase vs. cluster size. (d) Individual *in vitro* extracellular traces from a 9-AFE cluster & their average.

	[2]	[3-5]	[6]	[8]	**This work**
Technology (nm)	180	180	130	65	**180**
Target application	*In vitro*	*In vitro*	*In vivo*	*In vivo*	***In vitro & in vivo***
Recording type	Extracellular	Extracellular Intracellular	Extracellular	Extracellular	**Extracellular Intracellular**
No. electrodes	59,760	4,096	5,120	1,024	**6,144**
No. recording channels	2,048	4,096	384	1,024	**4,096**
No. stimulation channels	16	4,096	0	64	**4,096**
Recording power per channel (µW)	16	-	-	2.72	**5.7**
Total power per channel (µW)	42	305	95	24.08	**26.3**
Bandwidth (Hz)	1 – 10k	1 – 5k	0.5 – 10k	5 – 10k	**1 – 5k**
Input-referred noise (µVrms)	2.4 (300 – 10kHz)	5.6 (1 – 4.7kHz)	7.44 (300 – 10kHz)	8.98 (300 – 10kHz)	**7.4 (1 – 5kHz)**
ADC resolution sampling speed	10 bit 20 kSps/ch	Off-chip	14 bit 30 kSps/ch	10 bit 20 kSps/ch	**12 bit 10 kSps/ch**
Supply voltage (V)	3.3	3.6	-	2.5	**3.3**
Area per channel (mm²)	-	0.025	0.035	0.0062	**0.015**
Total chip area (mm²)	106.8	200	19.1	20	**144**

Fig. 6. Performance comparison.

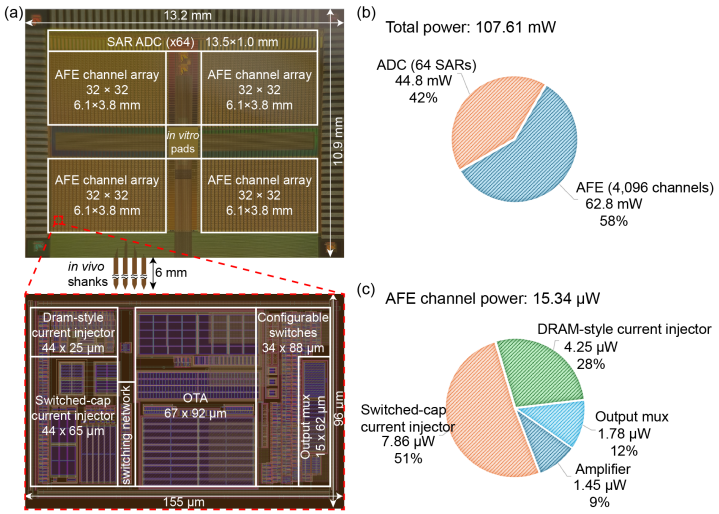


Fig. 7. (a) Die micrograph and AFE channel floorplan. (b) Measured chip power consumption. (c) Measured power consumption of single AFE channel.

Additional References:

[5] J. Wang et al., “Synaptic connectivity mapping among thousands of neurons via parallelized intracellular recording with a microhole electrode array,” Nat. Biomed. Eng, vol. 9, no. 7, pp. 1144–1154, Feb. 2025.

[6] S. Wang et al., “A Compact Quad-Shank CMOS Neural Probe With 5,120 Addressable Recording Sites and 384 Fully Differential Parallel Channels,” IEEE Trans. Biomed. Circuits Syst., vol. 13, no. 6, pp. 1625–1634, Dec. 2019.

[7] N. A. Steinmetz et al., “Neuropixels 2.0: A miniaturized high-density probe for stable, long-term brain recordings,” Science, vol. 372, no. 6539, p. eabf4588, Apr. 2021.

[8] D.-Y. Yoon et al., “A 1024-Channel Simultaneous Recording Neural SoC with Stimulation and Real-Time Spike Detection,” in 2021 Symposium on VLSI Circuits, Kyoto, Japan: IEEE, Jun. 2021, pp. 1–2.